ELSEVIER

Materials Science and Engineering B90 (2002) 25–33

MATERIALS SCIENCE & ENGINEERING B

www.elsevier.com/locate/mseb

Effect of the silicon nitride passivation layer on the Cu/Ta/SiO_2/Si multi-layer structure

Khin Maung Latt [a,*], H.S. Park [a], H.L. Seng [b], T. Osipowicz [b], Y.K. Lee [a], S. Li [a]

[a] *School of Materials Engineering, Nanyang Technological University, Nanyang Avenue, Singapore 639798, Singapore*
[b] *Department of Physics, National University of Singapore, Lower Kent Ridge Road, Singapore 119260, Singapore*

Received 21 May 2001; received in revised form 10 August 2001; accepted 15 August 2001

Abstract

Microstructure, composition and thermal stability of the SiN_x/Cu/Ta/SiO_2/Si (hereinafter 'passivated') multi-layer sample were investigated after annealing at different temperatures and compared with those of the Cu/Ta/SiO_2/Si (hereinafter 'unpassivated') multi-layer sample. Observed in this study were formation of new phases, movement of element atoms across the interface, failure of a tantalum (Ta) barrier layer, agglomeration of Cu grains and change in surface morphologies of nitride and Cu layers by Rutherford backscattering spectrometry, X-ray diffraction and scanning electron microscopy. The Cu layer of the passivated sample did not show a severe agglomeration phenomenon at high annealing temperature due to protection of the Cu surface from oxygen in the annealing ambient. In addition, there were no such phases as Cu_2O and Ta_2O_5 that were detected in the unpassivated sample. Although the thermal stability of the Ta layer was improved by addition of the passivation layer, Ta atoms diffused out to the passivation layer during annealing process at 750 °C, resulting in formation of Ta_2N at the SiN_x/Cu interface.

Keywords: Tantalum; Ionized metal plasma; Diffusion barrier; Metallization; Phase transformation; Interfacial reaction

1. Introduction

Recent research efforts have been focused on development of processes with which to utilize copper in place of aluminum as a conductor in microelectronic circuits. However, there are a number of issues that need to be addressed [1–4] before such a substitution can take place. Firstly, copper oxidation is not self-limiting and therefore some method of passivating the copper surface is needed. Secondly, adhesion at the copper/dielectric interface should be good and this interface must act as a diffusion barrier to transport of copper atoms from the metal lines into sensitive regions of the devices. A number of approaches have been investigated for passivation of the exposed Cu surface, including ion implantation, formation of surface silicides, treatment with organic inhibitors, annealing bilayer [4–7] and doping of the copper with metals [4,8–10]. Dielectric passivation films may be more favorable than others to suppress oxidation of the Cu surface because the process is easier and can be carried out with existing equipment. Silicon nitride is a typical dielectric material and has been extensively used in various technological areas, especially in the fabrication of microelectronic devices as an oxidation mask, a gate dielectric, an interlevel insulator, and a final passivation layer. All these applications are due to its remarkable properties such as high thermal stability, chemical inertness, extreme hardness, and good dielectric property. In this work, we have used the silicon nitride SiN_x layer for passivation of the copper surface.

The usual approach to resolve the adhesion issue is to insert a diffusion barrier/adhesion promoter between the dielectric layer and the copper. A variety of materials have been evaluated from low melting point metals [1,11,12] to refractory metals [4,13] to amorphous carbon [14] and several candidates have been proposed, including refractory metals (Ta and W) [15,16], nitrides (TiN and TaN) [17,18] and compounds (TiW and Ta–

* Corresponding author. Tel.: +65-7906161; fax: +65-7900920.
E-mail address: p101282@ntu.edu.sg (K.M. Latt).

0921-5107/02/$ - see front matter
PII: S0921-5107(01)00746-2

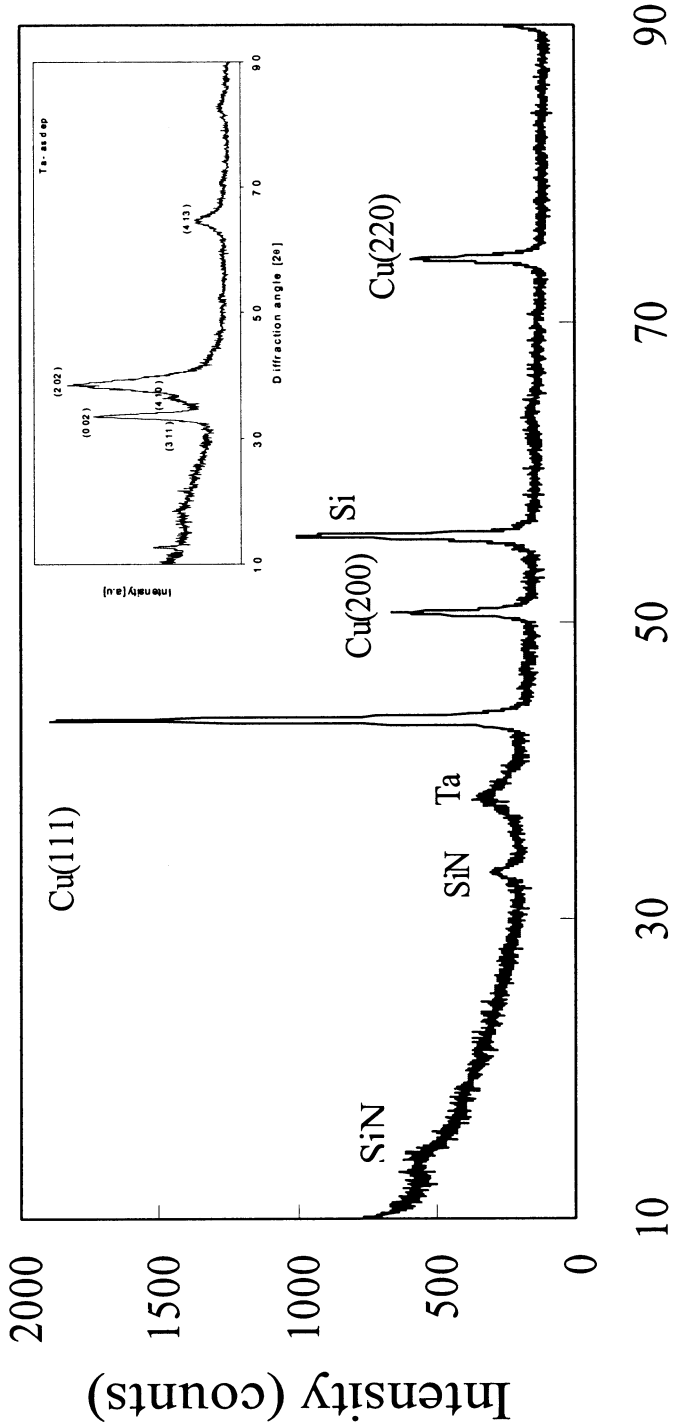

Fig. 1. XRD pattern obtained from the as deposited samples of Si_3N_4 coated Cu/Ta/SiO_2/Si multiplayer structure and the XRD pattern for as-deposited tantalum showing β-Ta (inset).

Si–N) [19,20]. Out of these candidates Ta has been widely investigated as a single metal diffusion barrier for the Cu metallization scheme, because it not only has both high melting point (2996 °C) and silicidation temperature (~ 650 °C), but it also shows a very low solubility limit in Cu [21]. In this study we have investigated the microstructure, composition, and thermal stability of the $SiN_x/Cu/Ta/SiO_2/Si$ multi-layer structure after annealing process at up to 850 °C

2. Experimental details

Sample preparation started with cleaning 8-inch bare Si wafers with (100) orientation in 10:1 diluted HF solution and rinsing in deionized water before SiO_2 deposition. A 500 nm thick PECVD SiO_2 layer was deposited with a gas mixture of SiH_4, O_2 and Ar at 350 °C. Subsequently the wafers were loaded into a cluster type of ionized metal plasma (IMP) sputtering equipment so that the Ta (30nm) layer and the Cu (200 nm) layer were deposited sequentially without vacuum break. Then, a PECVD SiN_x (20 nm) passivation layer was deposited with silane (SiH_4) and ammonia (NH_3) at 285 °C. The IMP and PECVD deposition process has been explained details elsewhere [22,23].

The samples were annealed for 35 min in N_2 ambient at an interval of 100 °C from 350 to 850 °C. X-ray diffraction (XRD) was used for analysis of both resulting phases and interdiffusion of the elements across the interface. The Cu–K_α X-ray ($\lambda = 1.542$ Å) scan was conducted from $2\theta = 20$ to 85° using a RIGAKU model RINT2000 diffractometer at a grazing incident angle of 2.5°, a scan speed of 4° min^{-1} and a 0.05° scan step. Surface morphologies of the layers were examined using JEOL 5410 scanning electron microscopy operated at 20 kV together with a Nanoscope III multimode atomic force microscope in tapping mode with silicon cantilevers at resonance frequencies in the range of 200–300 kHz.

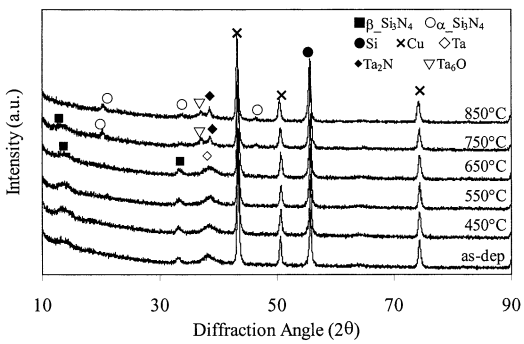

Fig. 2. XRD measurement results of $SiN_x/Cu/Ta/SiO_2/Si$ multilayer structure before and after annealing at various temperatures for 35 min in N_2 ambient.

Rutherford backscattering spectrometry (RBS) was employed to investigate diffusion behaviour of each element of the sample in conjunction with electrical measurements with a Four-point probe. Rutherford backscattering spectrometry (RBS) spectra were taken with 2 MeV He^+ ions at a scattering angle of 160° using a 50 mm^2 passivated implanted planar silicon (PIPS) detector of 13.5 keV resolution.

3. Results and discussion

Fig. 1 shows an X-ray diffraction pattern of the passivated multi-layer sample as deposited. The Cu film sputter-deposited on the Ta diffusion barrier has a strong (111) preferred orientation at 43.30°, while low-intensity peaks of (200) and (220) were observed at 50.43 and 74.13°, respectively. In contrast to sharp and strong Cu diffraction peaks, the low intensity reflection lines centered at 2θ angles of 13.439 and 33.153° can be indexed as β-Si_3N_4 (100) and (101) [24] showing crystalline structure since microstructure of SiN_x which depends on the deposited temperature was reported [25]. According to their results, the transformation from amorphous to crystalline structure for SiN_x films occurs the deposited temperatures in the range of 200–250 °C. The XRD pattern (inset) reveals that the peaks centering approximately at 33.55, 38.2 and 43.30° correspond to (002), (202) and (413) of the tetragonal β-Ta structure with a high-resistivity of 200 μΩ cm, respectively.

The XRD measurement, identified new phases formed in the passivated sample annealed at high temperatures, revealing interaction of the elements across the interface. As shown in Fig. 2, there are two new peaks, Ta_6O (001) at 38.80° and Ta_2N (111) at 38.90° [24], in the XRD patterns of the samples annealed at and above 750 °C. The solubility of oxygen in Ta of the body centered cubic (BCC) structure is high [26] and the incorporation of oxygen of more than 2–3 at.% in the Ta layer at high annealing temperatures leads to formation of the metastable Ta_6O oxide with small tetragonal distortion. Contrary to Ta_2O_5 phase formed in the $Cu/Ta/SiO_2/Si$ multi-layer sample above 650 °C [27]. Ta binds nitrogen from the SiN_x layer to form the Ta_2N phase. A β-Ta peak overlaps with those new peaks. A strong Cu (111) peak is shown at 2θ angles of 43.3° [24]. In contrast, any reaction among Cu, Ta, O and N was not observed in the samples annealed at and below 650 °C.

Upon annealing at 750 °C, a new low intensity peaks were appeared at 2θ angle of 20.680° which was identity as α-Si_3N_4 (101) and more peaks were observed at 38.535 and 36.53° which can be indexed as α-Si_3N_4 (102) and (220) [24]. This reveal the fact that β-Si_3N_4 has undergone a transformation into α-Si_3N_4 when annealing temperature higher than 750 °C since β-

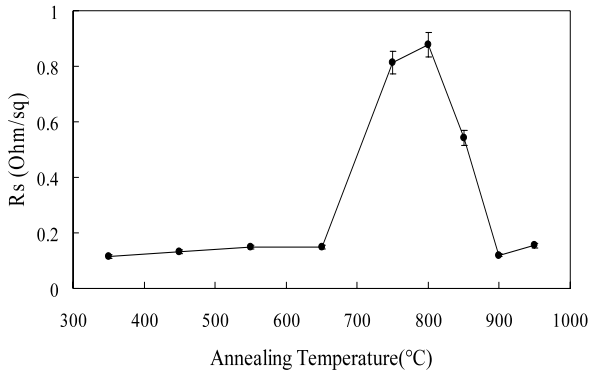

Fig. 3. Sheet resistance of Cu/Ta/SiO_2/Si multilayer structure as a function of annealing temperature.

Si_3N_4 was totally disappeared from the XRD spectrum. However, there is no significant change observed in Cu peaks after high temperature annealing process.

Fig. 3 shows a change in sheet resistance measured on the unpassivated sample as a function of annealing temperature. The sheet resistance value is determined almost by the copper thin film since it is much thicker (200 vs. 20 nm) and has a markedly lower resistivity (1.72 vs. 200 μΩ cm) than the Ta film and any other phases. Since the top Cu layer carries almost all the current, an increase in the sheet resistance can be assumed to reflect a microstructural or compositional change in the Cu layer. Hence, this curve can be used to estimate the degree of intermixing, reaction, or changes of integrity across the metallization layers as well. According to this figure, all samples, annealed up to 650 °C can maintain the same level of sheet resistance as the as-deposited sample. The abrupt rise in sheet resistance of the samples annealed at temperature higher than 650 °C for the unpassivated sample is primarily attributed to the penetration of Ta atoms into the Cu layer, resulting in intermixing with the Cu atoms. The surfaces of the samples appeared in patches after annealing at 750 °C for 35 min as in SEM observation (see Fig. 7). It is further evidenced by RBS spectrum (Fig. 4) in which a marked decrease in height of the existing Ta peak and the appearance of a new Ta peak at higher energy level. The concentration of Ta atoms at the sample surface annealed at 750 °C is a few orders higher in comparison to the sample annealed at 650 °C and the underlying films and/or a symptom of a catastrophic failure caused by an overall reaction involving all the metallization layers. The sheet resistance of the unpassivated sample drops down at annealing temperatures higher than 800 °C and returns to the level of the as-deposited sample at an annealing temperature of 900 °C. It is probably due to the phase transformation of β-Ta (tetragonal) to α-Ta (body centered cubic) since α-Ta phase has more than one order of magnitude lower resistivity compared to β-Ta (15 vs. 200 μΩ cm) [28,29].

The Cu_2O oxide found in the unpassivated sample [27] was not formed in the passivated one because oxygen atoms of the annealing ambient were prevented from directly reacting with the Cu layer. The mechanism of the Cu oxidation was studied by Li et al. [30]. It was observed that Cu was oxidized to Cu_2O at the temperature as low as 200 °C and then to CuO at 300 °C. Oxidation starts at the surface and progresses slowly into the bulk. Since the inward diffusion of oxygen proceeds gradually as a function of annealing time, the complete oxidation from Cu_2O to CuO depends on the extent to which oxygen is available for it. According to the XRD results of the Cu_2O phase was first detected upon thermal annealing at 750 °C and more Cu_2O found as the annealing temperature increased. However, the CuO phase did not show-up upon annealing even at higher temperature due to N_2 annealing ambient. Furthermore, any form of Cu oxide was not observed upon thermal annealing of the passivated sample.

Rutherford backscattering spectrometry (RBS) was used to examine migration of each element across the interface in the multi-layer sample upon annealing in N_2 ambient for 35 min at different temperatures. Fig. 4 shows the RBS profile of the unpassivated sample. The surface scattering energies for O, Si, Cu and Ta are indicated. The as-deposited films exhibit two inseparable Ta and Cu peaks without evidence of intermixing. The Ta layer appears to remain largely intact up to 450 °C. For the sample annealed at 550 °C, the motion of Ta atoms toward the Cu surface gradually begun, but the integrity of the structure is still remained. For the sample annealed at 650 °C (Fig. 4c), the motion of elements are more clearly observed and the RBS spectra show that the gradient of the trailing edge of the Cu signal changes and a small amount of Ta appears at the higher energy levels. The back edge of the Cu signal becomes more graded with increasing temperature (Fig. 4d), implying that Cu film starts to agglomerate, thus exposing Ta grains to the ambient.

Discrete peaks of Ta and Cu are clearly shown in the RBS profile (Fig. 5a) of the passivated as-deposited sample and do not change up to the annealing temperature of 650 °C. Upon annealing at 750 °C there is a shift of the Ta peak towards the surface. The occurrence of a small Ta peak at energy level of 1.836 MeV in Fig. 5c indicates that Ta atoms have diffused out to the Cu layer, unaffected by the presence of the SiN_x capping layer. They accumulated at the Cu/SiN_x interface and reacted with nitrogen, producing the Ta_2N phase during annealing at 750 °C. In contrast, the interface between the Ta layer and the SiO_2 layer remains smooth and intact throughout the same thermal annealing. For the samples annealed at 850 °C (Fig. 5d), movement of Ta atoms toward the Cu layer is more pronounced, which is evidenced by a reduction

of the Ta peak height as compared with the as-deposited samples and an appearance of a new peak at higher energy band. However, diffusion of Cu and Ta atoms into the SiO_2 layer was not detected (i.e. the formation of Ta_xSi_y and Cu_xSi_y).

It is important to know microstructure of the thin film because it plays an important role in deciding texture of the overlayer to be deposited on itself. AFM pictures are shown in Fig. 6 for the passivated sample as deposited. The 30 nm Ta film had a smooth and nonporous surface morphology, a surface roughness (rms) of ~ 0.29 nm and very fine grains with a mean grain size of ~ 10 nm as shown in Fig. 6a. The crystalline Cu layer, in Fig. 6b, exhibits small bumps with grain size of about ~ 80 nm and a roughness of ~ 1.309 nm. These bumps may correspond to the columnar structure of the film. The dielectric SiN_x layer deposited on Cu with $SiH_4/NH_3 = 1$ has a roughness of ~ 1.311 nm (Fig. 6c). Surface morphology of the silicon nitride film grown in island mode and composed of very fine particles.

Fig. 7 shows SEM images of the Cu surface of the unpassivated sample after different thermal treatments. A smooth and uniform surface of the as-deposited Cu film is shown in Fig. 7a. Similar surface images were observed for the samples annealed at temperatures lower than 500 °C. Upon annealing at 650 °C, it changes to a rough surface with small Ta grains dispersed between large Cu grains of about 1 μm (Fig. 7b). It can be supported with the RBS data (Fig. 4c) and a

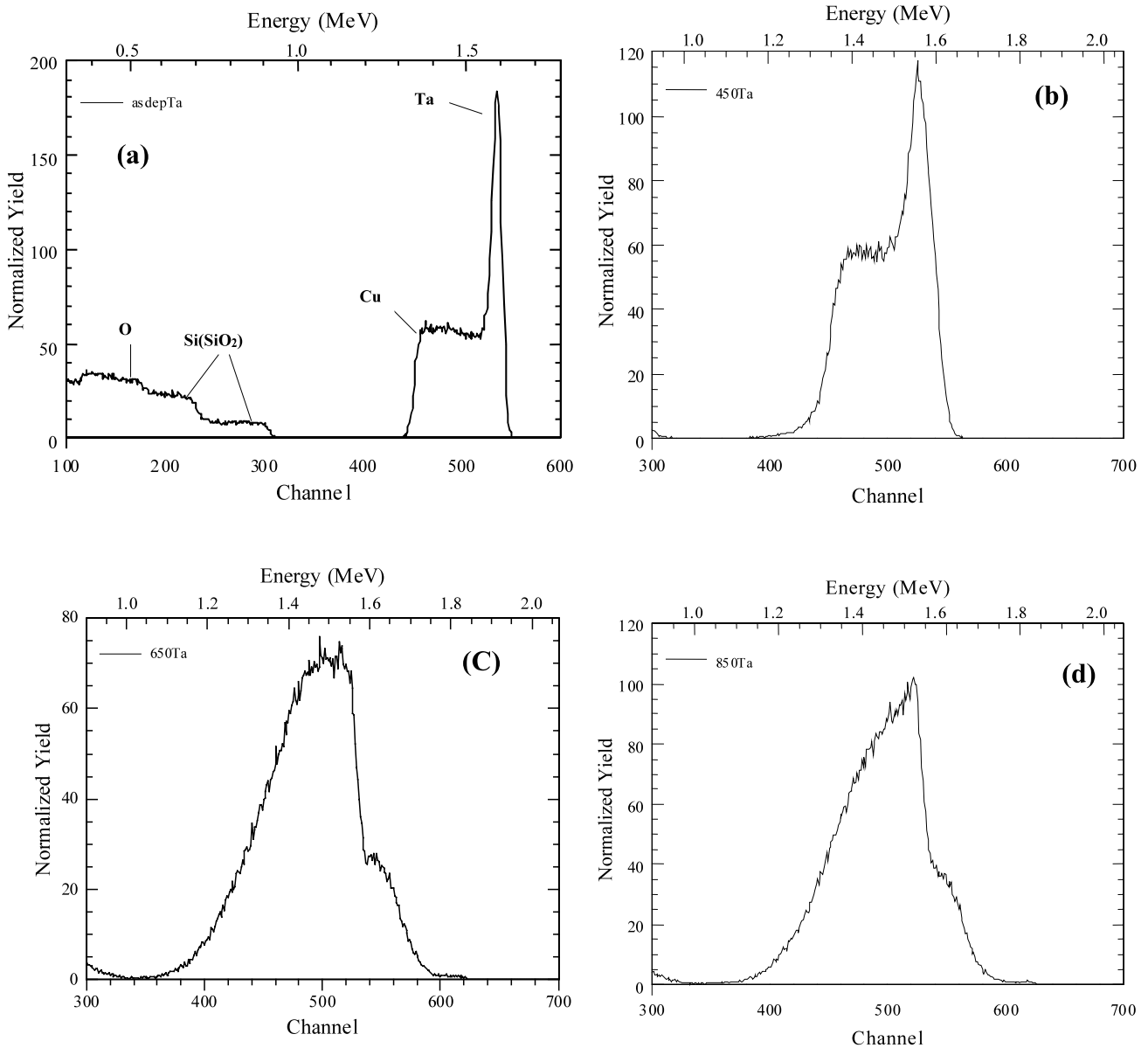

Fig. 4. 2 MeV H^+ RBS depth profile of the $Cu/Ta/SiO_2/Si$ multilayer structure annealed at various temperatures for 35 min in N_2 ambient.

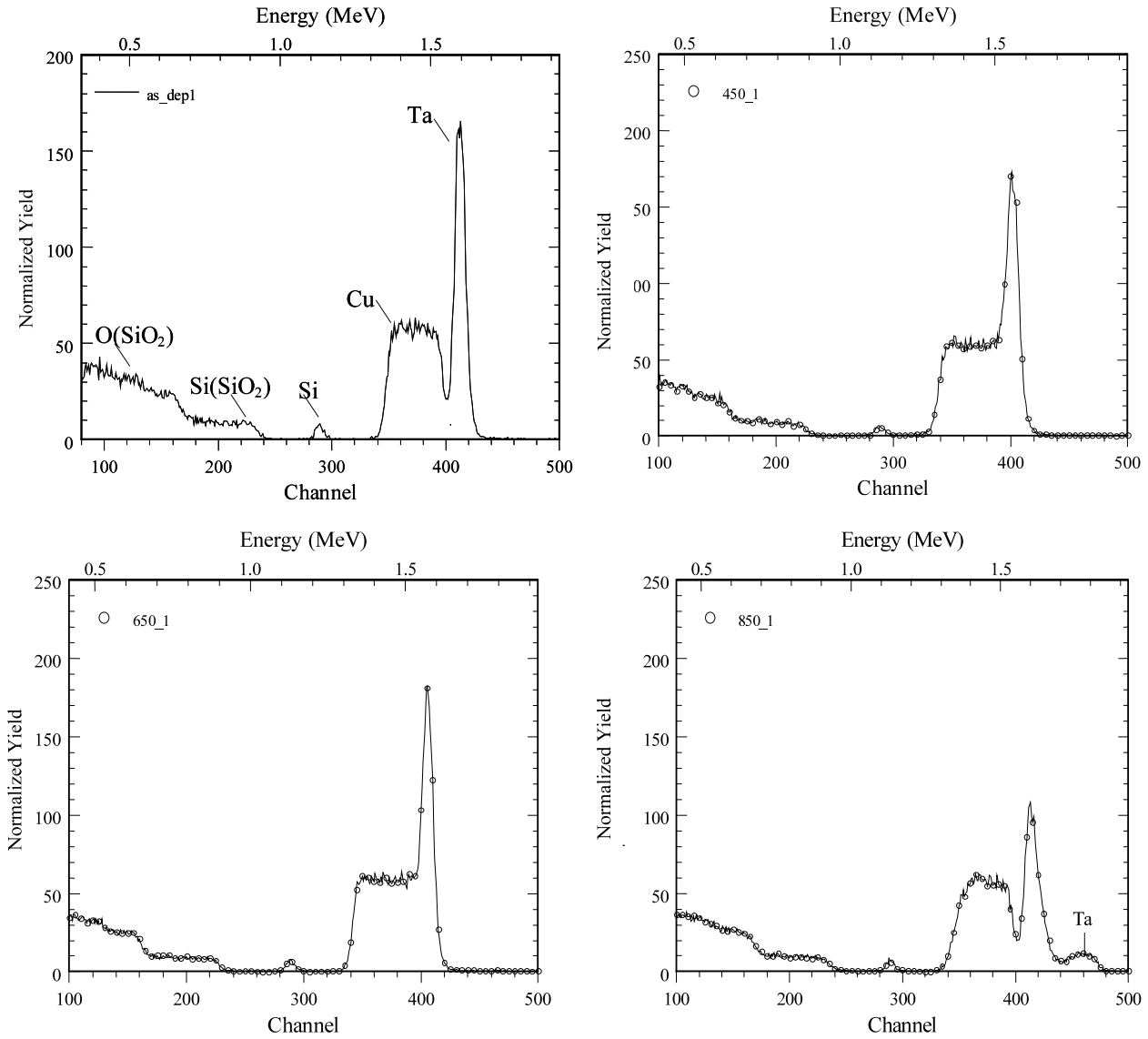

Fig. 5. 2 MeV H^+ RBS depth profile of the $SiN_x/Cu/Ta/SiO_2/Si$ multilayer structure annealed at various temperatures for 35 min in N_2 ambient.

sudden increase in sheet resistance (Fig. 3) of the same sample. During annealing treatment at 850 °C the Cu grains agglomerate into very big grains (Fig. 7c). Large Ta grains are conspicuously seen dispersed across the Cu surface. However, the Cu agglomeration phenomenon is not observed in the passivated sample due to isolation of the Cu layer from oxygen by the nitride passivation layer. No evidence of Cu agglomeration was observed in the RBS data of the passivated sample annealed even at 850 °C. Neither sample showed any peak of Cu_xSi_y phase resulting from diffusion of Cu through the Ta diffusion barrier.

Fig. 8 shows surface morphologies of the SiN_x layers in the passivated multi-layer samples. A smooth and uniform surface of the as-deposited SiN_x layer is shown in Fig. 8a. In contrast, a few ridges showed up on the nitride surface annealed at 650 °C and more pronouncing ridges/patches for the sample held at 850 °C (Fig. 8c). As the annealing temperature increases, out-diffusion of Ta atoms into the Cu film proceeds along the Cu grain boundaries due to its columnar structure. It has been explained in two ways. Firstly, the Cu layer has an average grain size of ~ 80 nm while Ta has a much smaller grain size, of the order of ~ 10 nm. Hence, it is easier for Ta atoms to migrate to the Cu film rather than Cu atoms to the Ta film. Secondly, it is still possible for Ta to diffuse outwards due to its high affinity with oxygen. Migration of Ta atoms to the Cu layer upon high temperature annealing leads to formation of a new (Cu–Ta) compound, $Cu_xTa_yO_z$, as evidenced by XRD analysis [27]. It is thought that Ta atom is the main moving element for the Ta_2N formation at the interface of SiN_x/Cu and Cu just offers short-circuit

diffusion paths for Ta to react with N atoms dissociated from the nitride layer. However, the sheet resistance of the sample remains unchanged up to annealing temperature of 650 °C. Below 650 °C a metastable TaO_x layer at the Ta/Cu interface effectively blocks Cu from moving into Ta as an additional barrier layer [31].

4. Conclusions

The effect of passivation layer of SiN_x on the thermal stability of $Cu/Ta/SiO_2/Si$ multilayer structure was studied before and after annealing and the failure mechanism was compared to the uncoated one. It was found that after passivated with SiN film, the

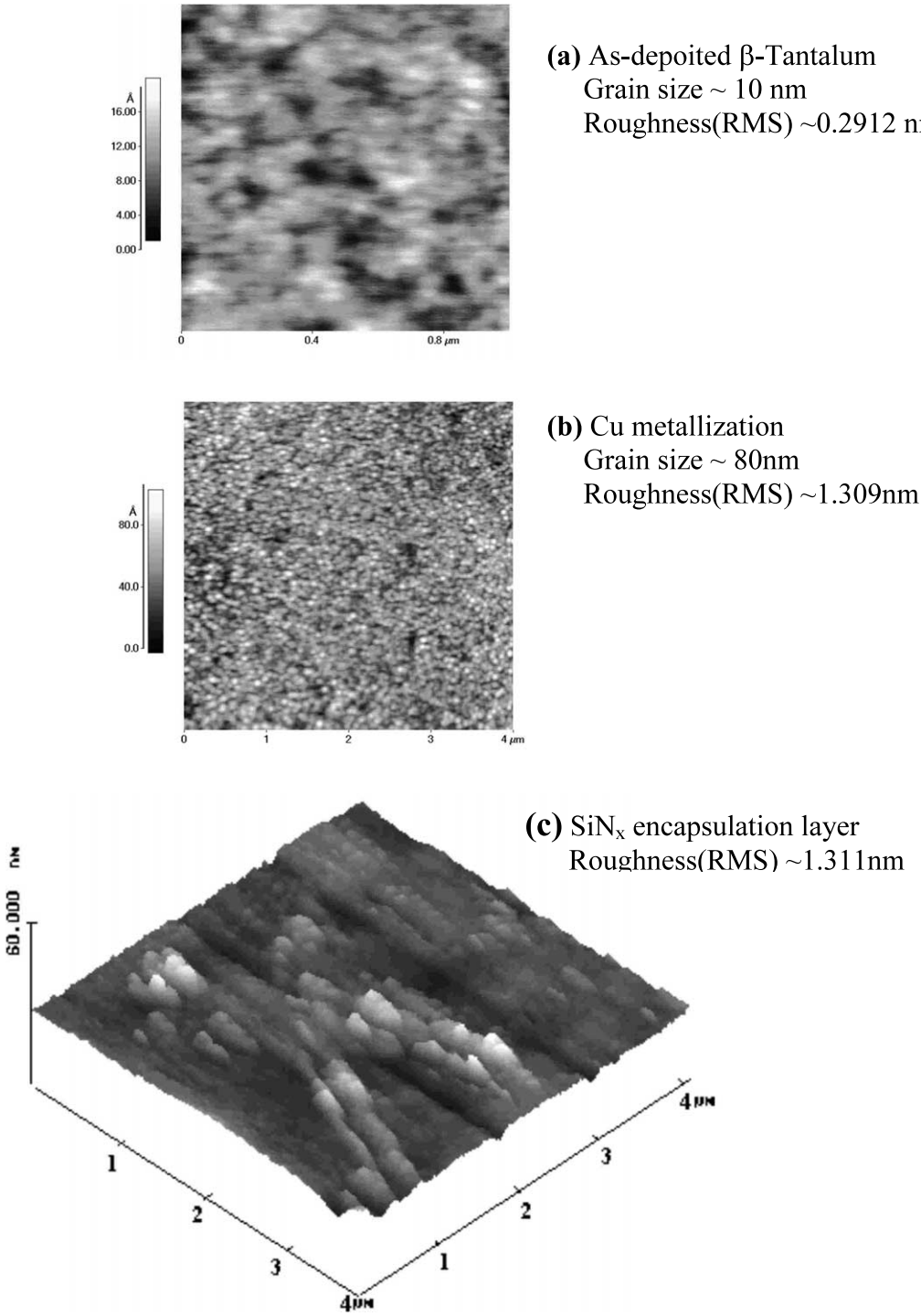

Fig. 6. AFM measurement result for SiN_x coated $Cu/Ta/SiO_2/Si$ multiplayer structures before deposition of the next subsequent layer (a) β-tantalum (b) Cu metallization and (c) the SiN_x encapsulation layer deposited on Cu.

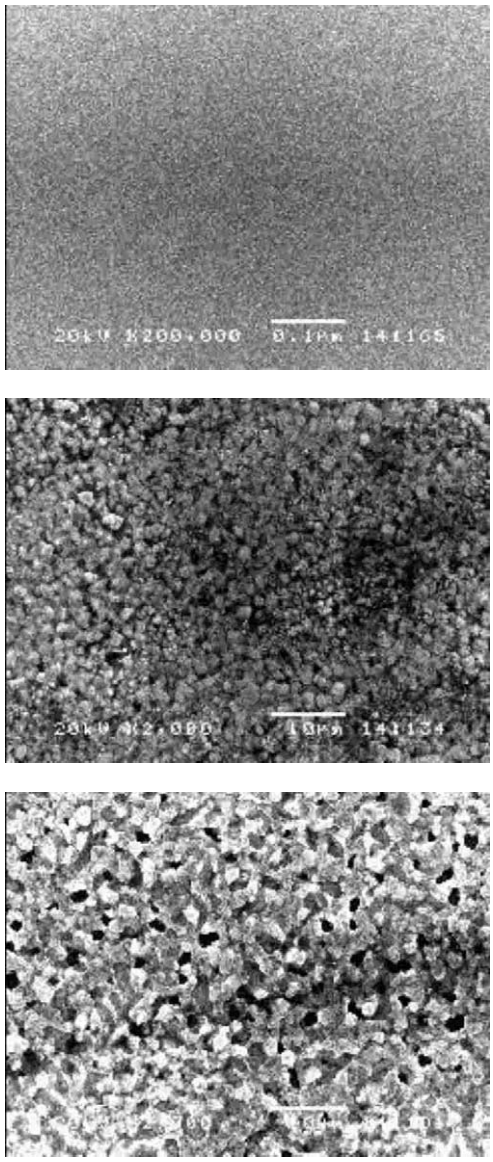

Fig. 7. SEM images of $Cu/Ta/SiO_2/Si$ multilayer structure before (a) and after annealing at (b) 650 °C and (c) 850 °C for 35min in N_2 ambient.

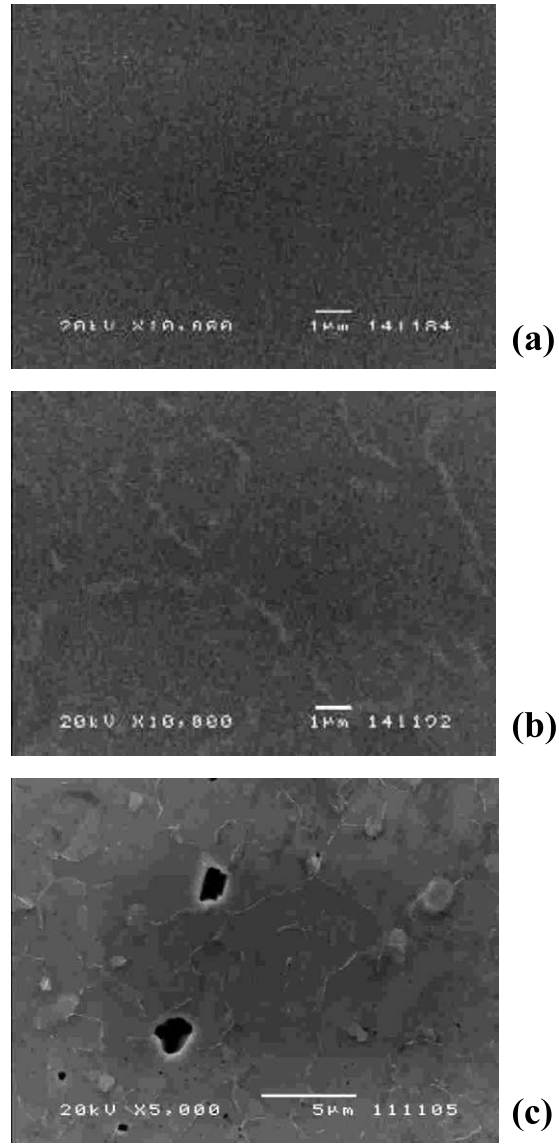

Fig. 8. SEM images of SiN_x on top of $Cu/Ta/SiO_2/Si$ multilayer structure before (a) and after annealing at (b) 650 °C and (c) 850 °C for 35 min in N_2 ambient.

formation of Cu_2O was not observed through out the annealing process. Ta_6O was formed only after 750 °C annealing instead of Ta_2O_5, which was found uncoated structure at the same temperature. But the reactions between Cu, Ta and O and the formation of $Cu_xTa_yO_z$ were fully suppressed in this $SiN_x/Cu/Ta/SiO_2/Si$ multilayer structure. The diffusion barrier found to be failed at 750 °C by out diffusion Ta atoms to the Cu layer and reacted with the dissociated N from SiN_x passivation layer and formed Tan. No further reactions were observed to taking place in the structure and no evidence of Cu diffusion through the Ta diffusion layer was found until after annealing at 850 °C. The passivation layer, SiN_x, after annealing at 850 °C clearly exhibited ridges and patches and grew as the annealing temperature increased.

References

[1] S.P. Murarka, R.J. Gutman, A.E. Kaloyeros, W.A. Lanford, Thin Solid films 236 (1994) 257.
[2] Y. Schacham-Diamand, A. Dedhia, D. Hoffstetter, W.G. Oldham, J Appl. Phys. Lett 60 (1991) 2983.
[3] S.P. Murarka, Metallization Theory and Practice for VLSI and ULSI, Butterworth, New York, 1992.
[4] J. Li, J.W. Mayer, Mater. Res. Soc. Bull. 18 (1993) 52.
[5] J. Li, P.F. Chapman, Y. Schachan-Diamand, J.W. Mayer, Advanced Metallization of ULSI 1992, MRS, Pittsburgh, PA, 1993, p. 75.
[6] J. Li, J.W. Mayer, E.G. Colgan, Appl. Phys. 70 (1991) 2820.

[7] H. Itow, Y. Nakasaki, G. Minamihaba, K. Guguro, H. Okano, Appl. Phys. Lett. 63 (1993) 934.
[8] J. Li, J.W. Mayer, Y. Schachan-Diamand, E.G. Colgan, Appl. Phys. Lett. 60 (1991) 2983.
[9] P.J. Ding, W.A. Lanford, S. Hymes, S.P. Murarka, J. Appl. Phys. 75 (1994) 3627.
[10] S.Y. Jang, S.M. Lee, H.K. Baik, J. Mater. Sci: Mater. Electron. Soc. 7 (1991) 271.
[11] B. Arcot, S.P. Murarka, L.A. Clevenger, J.M.E Harper, C. Cabral, Proceedings of the 9th VLSI Multiulevel Interconnection Conference, 1992, p. 306 (unpublished).
[12] R. Nadan, S.P. Murarka, A. Pant, C. Shepard, Mater. Res. Soc. Proc. 260 (1992) 929.
[13] L.A. Clevenger, N.A. Boharczuk, E. Holloway, J.M.E. Harper, C. Cabral, R.G. Schad, F. Cardone, L. Stolt, J. App. Phys. 48 (1993) 1331.
[14] R.G. Purser, J.W. Strane, J.W. Mayer, Proceedings of the Materials Reliability in Microelectronics III Symposium, MRS, Pittsburgh, PA, 1993, p. 481.
[15] C.A. Chang, J. Appl. Phys. 67 (1990) 6184.
[16] S.Q. Wang, I. Raaijmakers, B.J. Burrow, S. Suther, S. Redkar, K.B. Kim, J. Appl. Phys 68 (1990) 5176.
[17] K. Holloway, P.M. Fryer, C. Cabral Jr, J.M.E. Harper, P.J. Bailey, K.H. Kelleher, J. Appl. Phys. 71 (1992) 5433.
[18] S.Q. Wang, S. Suther, B.J. Burrow, C. Hoeflich, J. Appl. Phys. 73 (1993) 2301.
[19] P.J. Pokela, E. Kolawa, R.P. Ruiz, M.A. Nicolet, Thin Solid Films 203 (1991) 259.
[20] T.B. Massalski, Binary Alloy Phase Diagrams, 2nd ed., ASM/NIST, Metals Park, OH, 1986.
[21] K. Maex, M.V. Rossum, Properties of Metal Silicides, EMIS Data reviews Series No. 14, INSPEC, London, 1995.
[22] S.M. Rossnagel, J. Hopwood, J. Vac. Sci. Technol. B 12 (1994) 499.
[23] T. Lauinger, J. Moscher, A.G. Aberle, R. Hezel, J. Vac. Sci. Technol. A 16 (1998) 530.
[24] JCPDF cards no. Cu (040836), Ta_2N (260985), β-Ta (251280), β-Si_3N_4 (331160), α-Si_3N_4 (410360), Ta_6O (150206) and Si (261481).
[25] C. Ye, Z. Ning, M. Shen, S. Cheng, Z. Gan, J. Appl. Phys. 83 (1998) 5978.
[26] S.P. Garg, N. Krishnamurthy, A. Awasthi, M. Venkatraman, J. Phase Equilibrium 17 (1996) 63.
[27] Y.K. Lee, K. Maung Latt, K. JaeHyeong, T. Osipowizc, K. Lee, Mater. Sci. Eng. B68 (2) (1999) 99.
[28] H.-J. Lee, K.W. Kwon, C. Ryu, R. Scinlair, Acta Mater. 47 (15) (1999) 3965.
[29] K.M. Latt, Y.K. Lee, S. Li, T. Osipowicz, A.T.S. Wee, Int. J. Modern Physics B, in press.
[30] J. Li, J.W. Mayer, E.G. Colgan, J Appl. Phys. 70 (1991) 2820.
[31] T. Laurila, K. Zeng, J.K. Kivilahti, J Appl. Phys. 88 (2000) 3377.